Hindawi
Advances in Polymer Technology
Volume 2023, Article ID 3996687, 10 pages
https://doi.org/10.1155/2023/3996687

Research Article

Fabrication of Graphene Oxide Reinforced Biocomposite: Recycling of Postconsumed Footwear Leather

Rashedul Islam,[1] Md Ashikur Rahaman Noyon,[1] Thuhin Kumar Dey,[1] Mamun Jamal,[2] Rajasekar Rathanasamy,[3] Moganapriya Chinnasamy,[4] and Md. Elias Uddin[1]

[1]*Department of Leather Engineering, Faculty of Mechanical Engineering, Khulna University of Engineering and Technology, Khulna 9203, Bangladesh*
[2]*Department of Chemistry, Faculty of Civil Engineering, Khulna University of Engineering and Technology, Khulna 9203, Bangladesh*
[3]*Department of Mechanical Engineering, Kongu Engineering College, Erode, Tamilnadu, India*
[4]*Department of Mining Engineering, Indian Institute of Technology Kharagpur, Kharagpur, West Bengal, India*

Correspondence should be addressed to Md. Elias Uddin; eliasuddin@le.kuet.ac.bd

Received 4 April 2023; Revised 27 July 2023; Accepted 4 September 2023; Published 28 September 2023

Academic Editor: Dhanesh G. Mohan

The increasing concerns about solid waste disposal have led to the development of innovative strategies for repurposing waste materials. This paper describes a simple solution casting process for recycling postconsumed footwear leather fiber (PCF) into a biocomposite film reinforced with graphene oxide (GO) and polyvinylpyrrolidone (PVP). PVP was utilized as a compatibilizer to strengthen the interfacial bonding of GO and leather fiber via π–π interactions. UV–visible spectroscopy, Fourier transform infrared spectroscopy, X-ray diffraction, thermogravimetric analysis, and scanning electron microscopy were used to examine the material dispersibility bonding between GO and PCF, structural properties, thermal properties, and surface morphology of the biocomposite films, respectively. Compared to pure PCF film, the oxygen transmission rate of the prepared biocomposite films is elevated by 64% as well as the biodegradability rate is intensified up to 60%. In addition, the film's tensile strengths are raised by 216%, while their elongation at break is increased by 164.64% as compared with PCF. The versatility of these eco-friendly and biodegradable composite films extends to its possible applications in packaging and interior design. The outcomes of the research reveal the viability of manufacturing affordable and sustainable biocomposites through the utilization of waste leather from consumed footwear.

1. Introduction

Around the world, customers demand for fashionable footwear is gradually increasing to cope up with the current fashion trends [1]. As well as the change of consumers taste, the useable life of footwear is comparatively lower while rapid market fluctuations are also fortifying the progressive reduction of product lifespan. As a result, a huge amount of footwear is being dumped every year after its functional life. But the landfill sites are causing severe environmental pollution, including surfaces as well as groundwater through the leaching from decomposed waste [2]. Recently, incineration, mechanical breakdown, and biological treatment systems were introduced to minimize environmental impact. Despite having such compatible strategies, the concept of waste recycling has emerged to reuse the postconsumed footwear leather fiber (PCF) materials rather than direct disposal into the environment [3]. To ensure this, large footwear manufacturers such as Nike and SATCOL started programs to reuse the wastage footwear through a recycling process [4]. Staikos and Rahimifard [1] suggested the fabrication of the coverings for playgrounds and roads or as sound insulation from postconsumed footwear waste. To address the issue of environmental pollution, leather solid waste from tannery or other leather industry are incorporated with different binders and filler such as polycaprolactone (PCL), polylactic acid, nanomaterials, natural rubber latex, linear low-density polyethylene (LLDPE), polyvinyl alcohol (PVA), and so forth to fabricate composite

materials. The well dispersion and distribution in the polymeric matrix and high degree of interaction are the two primordial conditions for obtaining composite materials [5]. Leather solid wastes were used as fillers in fabricating composites, which are potential, conducive, and cost-effective. Those composite materials are being used as heat insulators, sound insulators, interior moldings for automobiles, soles and mid soles of shoes as well as packaging materials. Composite films were fabricated from leather solid waste incorporated with LLDPE, which possess moderate mechanical properties [6]. Composite sheets were fabricated from leather solid waste incorporated with natural rubber latex [7]. Biodegradable composite materials were produced from leather trimmings with PVA and PCL, but it exhibits poor mechanical properties [8]. On the other side, nanofillers such as graphene, carbon nanotubes, hydroxyapatite, clay, and so forth are being used in nanocomposite technology with low loading, which has already been certified to produce new materials with high performances and specific properties [9]. Among the above nanofillers graphene oxide (GO) is one of the promising nanofillers, which has both dispersion and interaction magnitude [10, 11].

GO is a single-layer atomic-thick structural films with different functional groups (hydroxyl, carbonyl, carboxyl, and epoxy). This is used in different applications owing to its significant properties including more mechanical strength, thermal stability, antioxidant properties, and larger surface area (2,418 m^2/g) [12, 13]. More specifically, these nanomaterials are frequently applied in such functions where larger surface area and material strength are required. They are the most concerning issues including polymer composites, energy storage, water purification, and catalysts [14–16]. In terms of dispersibility, oxygen-containing groups made GO more hydrophilic and causing the easy dispersion in water media with proper exfoliation rather agglomeration [17]. Therefore, GO is a promising nanofiller for improving the properties of composites. Additionally, El Achaby et al. [18] prepared bionanocomposite film with extraordinary properties by incorporation of GO in CS-PVP blend [19]. Then, Mahmoudi et al. [20] fabricated antimicrobial, transparent nanocomposite through GO in CS-PVP blend. In those composites, polyvinylpyrrolidone (PVP) was used as compatibilizer with film-forming ability and nontoxic behavior. It is a long-chain, well-defined, structured synthetic polymer with a *N*-vinylpyrrolidone monomer [21]. Besides, Pandele et al. [22] and Panda et al. [23] successfully prepared nanocomposite films with good mechanical strength and biocompatibility properties on incorporation of GO in CS-PVA blend as well as starch-PVA composites films were prepared. Moreover, Rodríguez-González et al. [24] developed biocomposites of CS-starch and carboxymethyl cellulose–starch blends reinforced with GO and keratin-grafted GO. It was noticed in these studies, with addition of GO the thermomechanical properties of the composites were notably enhanced.

This study introduces a novel and cost-effective method for producing environmental friendly biodegradable composite films from PCF and GO, where PVP was used as compatibilizer. The dispersibility, bonding, thermal stability, surface morphology, and mechanical strength of the fabricated composite films were ensured through UV–Vis spectroscopy, Fourier transform infrared spectroscopy (FTIR), thermogravimetric analysis (TGA), scanning electron microscopy (SEM), and tensile test, respectively. Moreover, gas barrier properties and biodegradability of the composite films were also investigated through oxygen transmission rate (OTR) and soil burial test. The characterization results indicate that the fabrication of PCF/GO composite films from postconsumer waste leather fibers and GO represents a significant step forward in producing environmentally sustainable packaging and interior decorating materials.

2. Materials and Methods

2.1. Materials. Postconsumed waste footwear leather was collected from the dumping site of Khulna City Corporation, Bangladesh. All of the analytical graded chemicals including PVP, natural graphite flakes, dimethylformamide solution, sodium nitrate, potassium permanganate, hydrogen peroxide, hydrochloric acid, and sodium hydroxide were purchased from Sigma–Aldrich, Bangladesh through a local supplier of Khulna city.

2.2. Methods

2.2.1. Preparation of Graphene Oxide from Natural Graphite Flake. In this experiment, natural graphite flake (crystalline, 300 mesh) was used to prepare GO via modified Hummer's method [25]. Around 2 g of graphite flakes were dispersed in 46 mL of H_2SO_4 (95%) to prepare a homogeneous suspension through rigorous mixing in ice-water bath (~5°C) for 30 min. At the same time, 2 g of $NaNO_3$ and 12 g of $KMnO_4$ were added into the solution dropwise and stirred for 2 hr in the ice-water bath. Simultaneously, 12 g of $KMnO_4$ was mixed slowly to the suspension and stirred for 2 hr. After removing it from the bath, the suspension was stirred again at 35°C in a preheated oil bath for 6 hr. With the progress of reaction with time, the solution was successively turned into a colloidal paste-like appearance and seemed to be brownish in color. Then, 92 mL of deionized (DI) water was added carefully to the mixture and stirred for an additional 2 hr. Subsequently, 280 mL of DI water was mixed again and followed by 35% of hydrogen peroxide until turns to golden yellow. To remove unwanted impurities, the mixture was centrifuged with 5% HCl and rinsed with DI water several times to confirm the neutral pH of the solution. Finally, the desired amount of GO was dispersed in DI water (1 mg/mL) and sonicated for 30 min and centrifuged to remove the unexfoliated part. The resultant was contained stable dispersion of GO and it was collected through freeze-drying.

2.2.2. Extraction of Leather Fiber from Footwear. At the initial stage, abandoned collected footwear leather waste was washed properly and dried in an oven at 60°C to remove moisture for 2 hr. Then the sample (3 g) was shredded into small pieces and hydrolyzed in alkali media (150 mL, 1.0 N NaOH) and stirred at 80°C for 3 hr owing to complete and uniform digestion of leather fiber [26]. After that, the sample was cooled at room temperature, filtered to collect residue,

Table 1: Blended films composition.

Sample name	Composition
S_1	100% PCF + 0% GO
S_2	95% PCF + 5% GO
S_3	90% PCF + 10% GO
S_4	85% PCF + 15% GO
S_5	80% PCF + 20% GO

and washed thoroughly to remove the unwanted alkaline solution. Finally, the residue was placed in a petri dish and heated in an oven at 70°C until it was properly dried. Subsequently, desiccation was also performed to completely remove any residual moisture.

2.2.3. Preparation of GO–Leather Fiber-Based Composite. At first, the hydrolyzed leather fiber (PCF) was dissolved in water and sonicated for 2 hr. A fixed amount of PVP (3 g) compatibilizer was separately dissolved in 150 mL DI water with constant stirring for 1 hr and mixed thoroughly. Then, the obtained solution of PVP was added to the PCF solution followed by mechanical stirring for 2 hr to confirm proper mixing. For the preparation of GO-based composite films, the desired amount (5, 10, 15, 20 wt% in regard to PCF) of synthesized GO was dissolved in water via sonication for 1 hr to maintain homogeneity. Then, these solutions were mixed in PCF slowly and sonicated again for 2 hr to acquire a proper homogenous solution. Then, the mixer was refluxed at 80°C with 24 hr [27]. At last, the solution was filtrated and dried in an oven at 70°C to prepare the final composites. The composite films were prepared using different amounts (0%, 5%, 10%, 15%, and 20%) of GO with PCF and designed as S_1, S_2, S_3, S_4, and S_5, respectively. The compositions of blended films are shown in Table 1.

2.2.4. Characterization of Composite. UV–Vis spectroscopy was conducted to check the dispersibility of nanomaterial in water by using a UVS-2100 SCINCO spectrophotometer. X-ray diffraction (XRD), FTIR and TGA were investigated to inspect the structural properties, functional groups, and thermal stability of composite via D/Max 2500 V/PC (Rigaku Corporation, Tokyo, Japan) (Cu K$\alpha \sim 0.1541$ nm) at a scan rate of $2°(2\theta)$ min^{-1}, NICOLET 6700 FTIR instrument (Thermoscientific, USA) in the frequency range of 500–4,000 cm^{-1} and TGA was performed using high resolution 2950 TGA thermogravimetric analyzer according to ASTM E1131 standard method, respectively. Moreover, SEM and OTR were also carried out to analyze the structure and gas barrier properties of GO-based biocomposite through the utilization of JSM-7800F, JEOL, and ASTM D3985, respectively. At the last stage, tensile strength, as well as percentage of elongation, were tested by SATRA TM137. Biodegradability of fabricated composite and PCF were studied according to Chiappero et al. [28]. Samples were collected and specimens were cut into a size of 2×2 cm^2. The precisely sized specimens were then buried in the soil of a plant pot. Water was regularly added to the soil at room temperature to maintain the appropriate level of humidity.

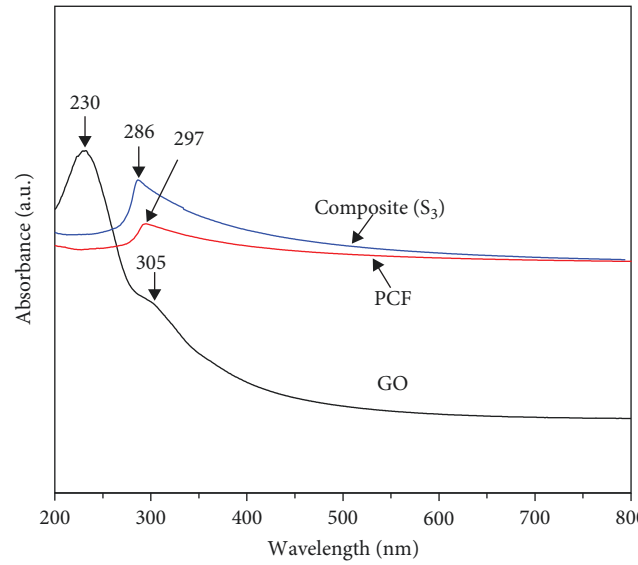

Figure 1: UV–Vis spectroscopy of pure GO, PCF, and composite (S_3).

The specimens were brought out from the soil, washed with clean water, and dried for 30, 60, 90, and 120 days, respectively. In the soil burial biodegradability test, the weight loss percentage for each sample was calculated.

3. Results and Discussion

3.1. UV–Vis Spectroscopy. Figure 1 shows the UV–Vis spectra of pure GO, PCF, and composite (S_3). A strong peak at ~230 nm corresponding to the π–π transition of C = C and a small peak at~305 nm attributed to the $n \longrightarrow \pi^*$ transition of C = O were indicating the presence of oxygen-containing functional groups in GO [29]. In view of PCF, the broad peak at 297 nm was noticed, which confirms the presence of tanning agents in dispersing media [30]. However, both of these peaks from GO were absent in the case of S_3 and a peak was shifted from 230 to 286 nm due to the increase in absorbance and it signifies dispersion characteristics of the S_3 [31].

3.2. FTIR Analysis. The FTIR spectra of GO, PCF, and composite (S_3) are presented in Figure 2. The FTIR spectrum of GO is indicating the presence of different oxygen-containing functional groups such as a broad band at ~3,435 cm^{-1} denoting the O–H stretching vibration of hydroxyl groups [32]. The peak at ~1,733 cm^{-1} is presenting C = O moiety of –COOH groups and the peak at ~1,634 cm^{-1} is highlighted for intercalated water molecules or unoxidized graphitic domain. Moreover, the band at ~1,061 cm^{-1} is described for epoxy stretching. In addition, peaks at ~1,396 cm^{-1} is appeared O–H deformation [26]. In respect of PCF, broader peaks have appeared at 3,453 and 603 cm^{-1} for H_2 bonded –OH stretching vibration and –NH group vibration in fibrous material, respectively [33, 34]. Moreover, peaks at ~1,657 and ~1,385 cm^{-1} appeared for amide I, and amide III absorption peaks of collagen fibers, respectively [35]. With regards to the S_3, some distinct peaks were observed at 2,955, 1,269, 1,090, and 1,014 cm^{-1}. These peaks were

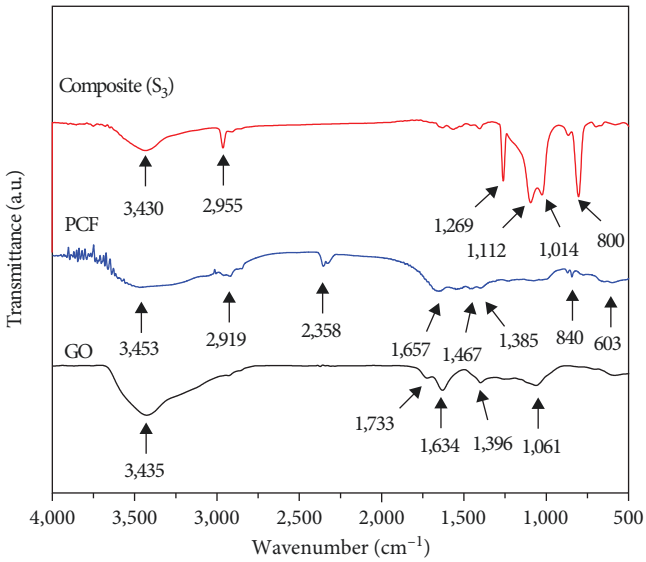

FIGURE 2: FTIR spectra of pure GO, PCF, and composite (S_3).

shifted and intensified, indicating interactions between GO and the collagen in PCF. These peaks were attributed to the shifting of functional groups in the S_3, including –NH group vibrations, epoxy groups, and O–H deformation.

3.3. Thermal Analysis. For hydrothermal stability test of PCF, GO, and composite (S_3), TGA and derivative thermogram (DTG) was performed and shown in Figure 3. The DTG analysis of PCF, GO, and S_3 revealed a two-stage degradation process. It helped to identify decomposition peaks, providing insights into the composite's (S_3) stability and thermal behavior. The curves revealed a gradual 5% weight loss in PCF at 50–100°C, attributed to water and moisture removal. Furthermore, a significant 35% mass reduction occurred between 400 and 500°C, indicating the breakdown of collagen structure and degradation of tanning materials in PCF. These observations provide valuable insights into the thermal behavior and composition of the material [36]. In the case of GO, two distinct decomposition points were identified. The first point was 8% weight loss at 50–100°C caused by the loss of absorbed water. The second point was a 40% weight loss at 150–210°C due to the decomposition of various oxygen-containing groups [18]. On the other hand, the temperatures of degradation for S_3 is shifted toward the high temperatures with a minimum weight loss (2%, 25%) at 50–100°C, 450–550°C, respectively, as identified in the two steps of degradation, which gives advantage to improve the thermal stability of these S_3 films. Therefore, maximum temperature for degradation and lower mass weight loss was observed in the analysis of S_3 film for the sequence of the hydrogen bond network formation between negatively charged functional groups of GO and positively charged side chain amino functional groups of collagen fibers of PCF as illustrated in the FTIR spectra analysis. So, it can be explained that a possible mobility suppression of the PCF segments by embodied of GO is appeared.

3.4. SEM Study. The morphology and structure of GO, PCF, and composite (S_3) are characterized using SEM and the respective images are shown in Figure 4. The excellent dispersion and smooth surface of GO is observed in Figure 4(a). The surface of PCF demonstrates a typical fiber-like, irregular ribbon structure with a smooth surface and having agglomeration due to a strong bonding effect such as hydrogen bonding between fibers [37]. In case of S_3, it was observed that GO are densely packed on the surface of the irregular and flake-like leather fiber films and a new uniform morphology was infused due to the strong interfacial interaction between GO and leather fiber. In addition, a cross-sectional image of S_3 is presented in Figure 4(d). It is evident from the figure that graphene sheets remained well dispersed throughout the matrix in the S_3. Moreover, these may happen due to the low molecular weight of PVP, which acts as a compatibilizer with the increment of matrix chain mobility [38]. However, the morphological observations described above are consistent with the mechanical properties of the S_3, as evidenced by the tensile properties of the materials.

3.5. XRD Analysis. In order to apprehend the crystal structure of the composite (S_3) films and PCF, also to look into the exploitation of GO within the composite, the samples were analyzed through XRD which is shown in Figure 5. The as-prepared GO showed a broad peak at 2θ of around 10.10° with an interlayer spacing of 0.83 nm. This confirmed that graphite was well oxidized to produce GO [39]. Effective dispersion of GO may be achieved due to its surface's abundance of oxygen-containing functional groups and the electrostatic repulsion between negatively charged GO sheets [40]. The XRD characteristics of PCF showed the presence of the broad peak at around 24.45° and 42.80° in which these peaks correspond to the hydrated crystalline structure and the existence of an amorphous structure. XRD analysis of the PCF shows that the structure is semicrystalline and the sharp peaks observed around 42.80°, indicating the average intermolecular distance of the amorphous part regenerated from the PVP. Regarding S_3, a broader peak with a 2θ value in the range of 15°–28° revealed the absence of the peak corresponding peak to GO ($2\theta = 10.10°$) [41]. The XRD analysis of S_3 indicated that GO is totally exfoliated in the composite matrix. Besides, the high consistency between GO and the PCF matrix is responsible for limiting the rearrangement of sheets into the layered structure of graphite oxide. Over and above, after addition of GO the S_3 shows a structure similar to that of PCF, indicating that the structure of composites is not affected by GO.

3.6. Biodegradability Test. Figure 6 shows the weight loss percentages after soil burial tests for PCF and fabricated composite films. The observation of degradation under soil was done for 120 days, where the samples were checked for weight loss at every 30-days interval. Three random strips of dimension $2 \times 2\ cm^2$ were cut from pure PCF and S_3 and the results are given as mean of three samples, whereas PCF film was used as a control. The degradation rate was nearness

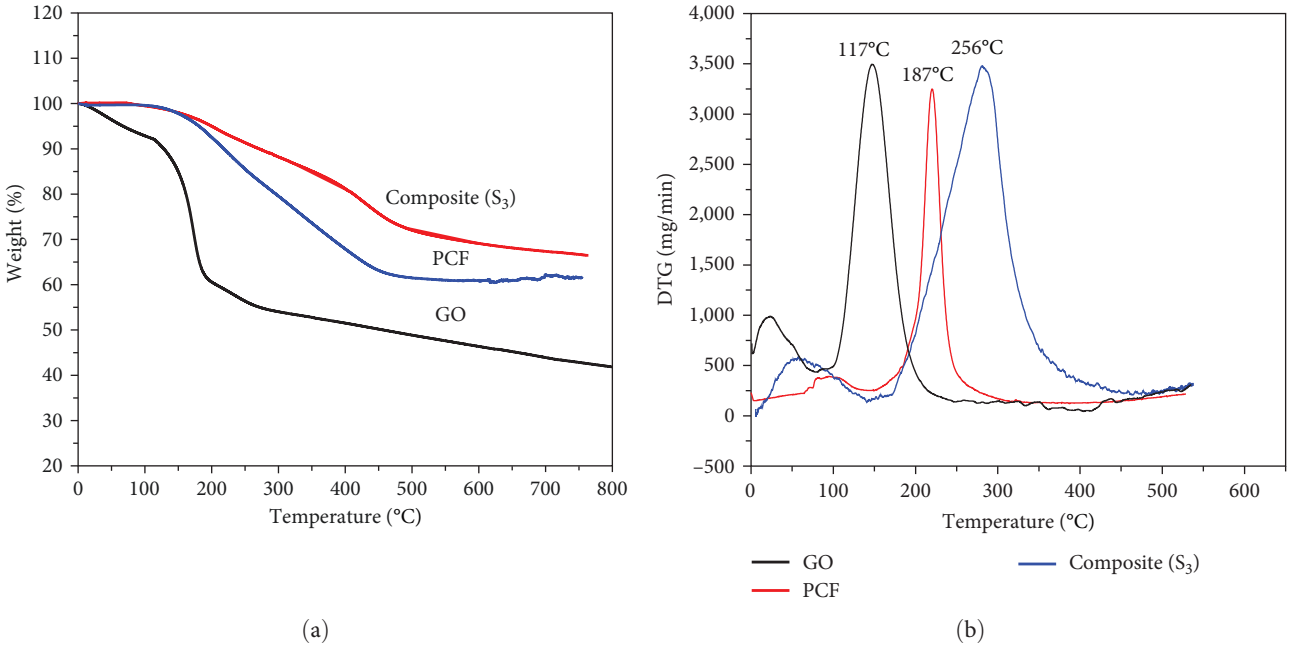

Figure 3: (a) TGA and (b) DTG analysis of GO, PCF, and composite (S_3).

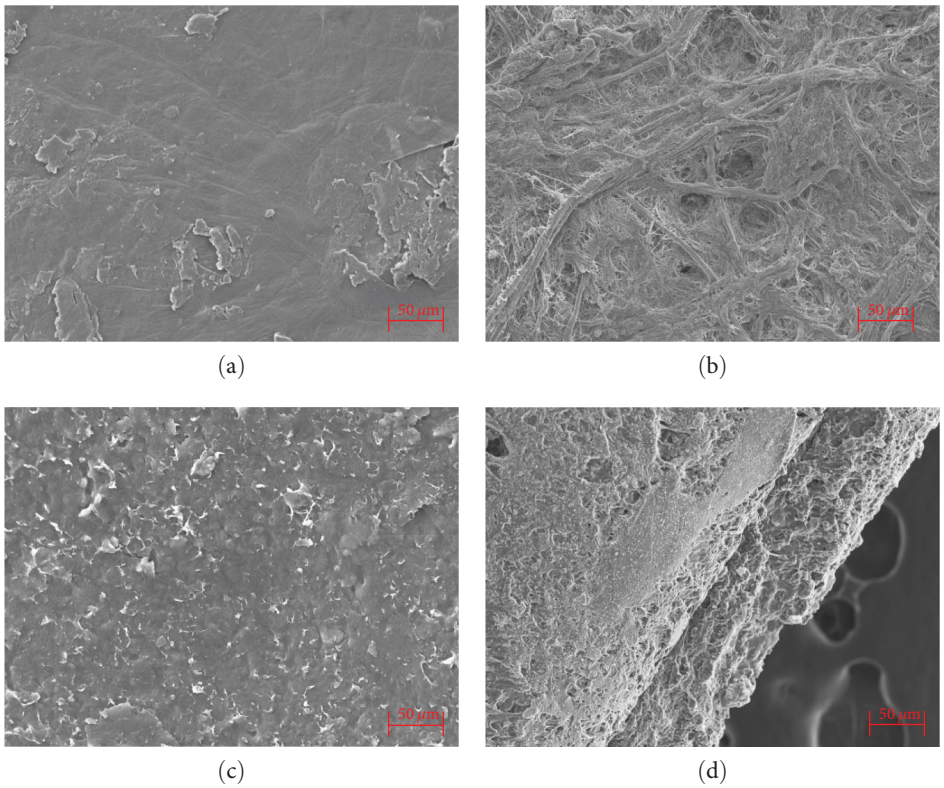

Figure 4: SEM study of (a) GO, (b) PCF, and (c, d) (S_3) (surface and cross-section).

similar for both the PCF and S_3 in the first 30 days. The rate of degradation for biocomposite film (S_3) was consistently enhanced through the next 30 days. The overall surface of the film was found to be shrunken. On comparison to PCF film, the S_3 showed the maximum rate of degradation of 60% on 120th day and there was no further weight loss recorded after 120 days. This saturation in degradation rate could be attributed to the difficulty in breaking down ester linkages by citric acid. The protein-enriched S_3 was observed to more amenable source for the soil bacteria than PCF films. The vital cause

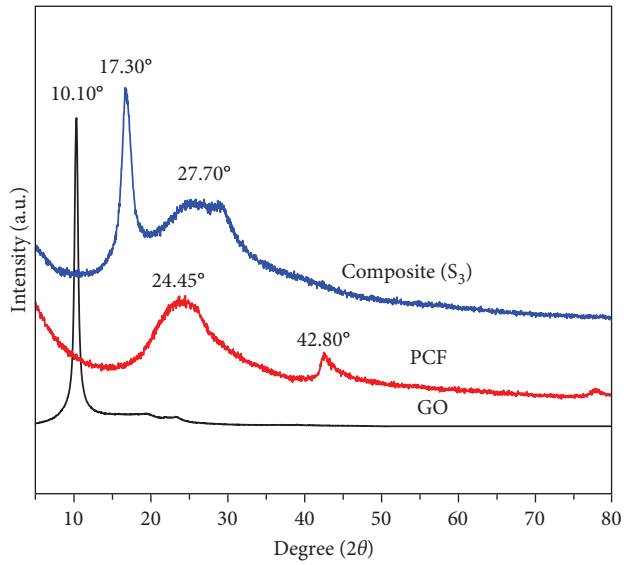

Figure 5: XRD analysis of pure GO, PCF, and composites (S_3).

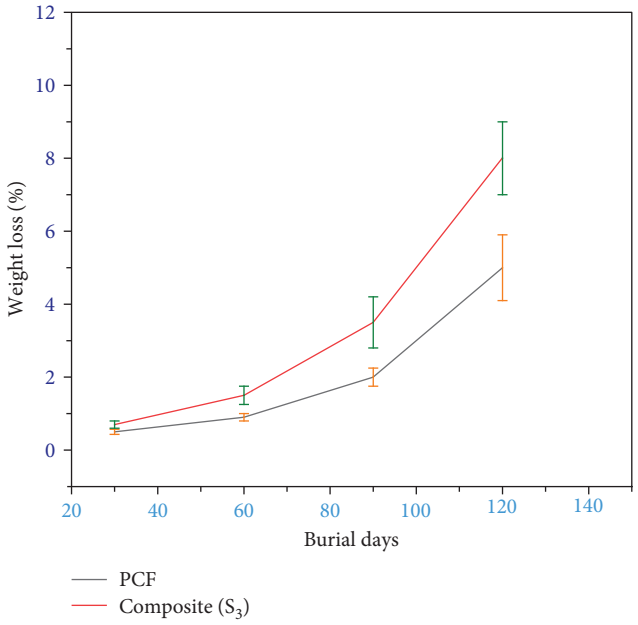

Figure 6: Biodegradability test by soil burial of PCF and composite (S_3).

for the increased biodegradability of fabricated composite film S_3 was a favorable hydrophilic condition by incorporating GO in PCF which is suitable for increasing enzymatic activity by different microorganisms [42].

3.7. Oxygen Gas Barrier Properties. The OTR of PCF and composite (S_3) is depicted in Figure 7. To enhance the gas barrier properties of fabricated composite, alternation of gas molecules is highly significant to consider. But in the case of leather-like fibrous material, gas barrier capacity is quite low in the dry state. So the infusion of GO-like impermeable nanomaterial can enhance the barrier property through uniform distribution as well as proper orientation in the host

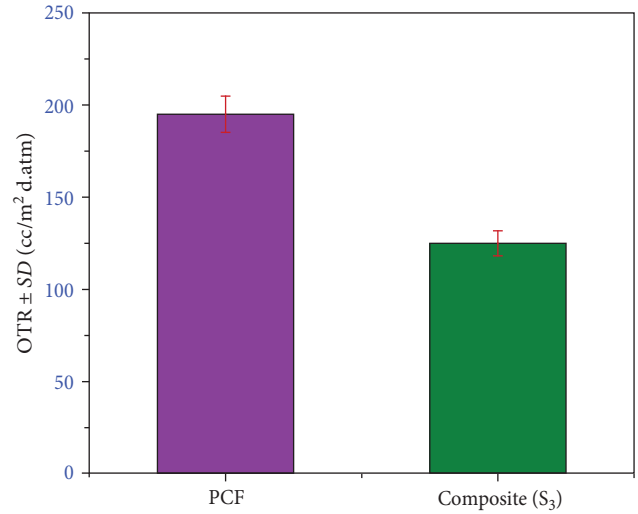

Figure 7: OTR analysis of PCF and composite (S_3).

Table 2: Mechanical properties of fabricated composite films.

Sample name	Tensile strength (MPa)	Elongation (%)
S_1	47.13 ± 3.5	25.20 ± 1.9
S_2	103.45 ± 8.8	47.48 ± 3.1
S_3	149.00 ± 12.7	66.69 ± 4.8
S_4	113.49 ± 9.3	58.75 ± 3.9
S_5	73.63 ± 5.9	42.45 ± 2.7

matrix of composites [43]. From the result of OTR, the key function of nanofillers (GO) is to block the gas molecule diffusion with higher tortuosity, which causes the longer and tortuous diffusive pathway for gas molecules and resulting in improved gas barrier properties than pure material-based films [44, 45]. In consequence, the OTR value of PCF (~195 cc/m^2·d·atm) was higher at the initial stage. But after grafting with GO, the OTR value of S_3 was decreased up to ~125 cc/m^2·d·atm, which represents the 64% increase in the gas barrier properties after incorporation of GO in composite fabrication. Therefore, this improvement significantly indicates the eventual distribution of GO as well as the reduction of intermolecular gap within composite materials. This behavior can be explained in terms of the homogeneous dispersion of GO, which creates a tortuous path for the penetration of earth material and limits the gas passing properties of the produced composites, which is most suitable condition for its potential application as packing material [46].

3.8. Tensile Strength and Percentage of Elongation. The mechanical properties of the pure PCF film (S_1), PCF with GO (S_2, S_3, S_4, and S_5) were investigated by tensile testing machine. The tensile strength and the percentage of elongation of the fabricated films are presented in Table 2. The tensile strength represents the maximum stress value applied to the material and percentage of elongation is defined as the strain to break off the material. From the table, the S_1 has an elongation of 25.2%, tensile strength of 47.13 MPa in the absence of GO. After that, adding GO nanomaterials the

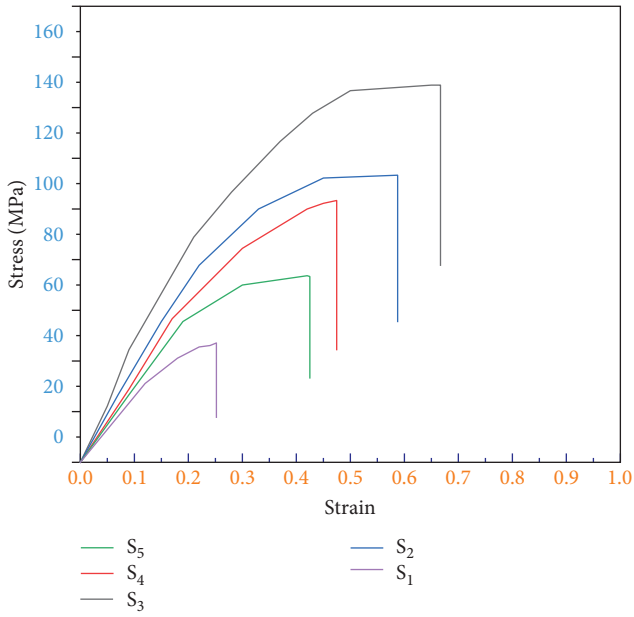

FIGURE 8: The stress–strain curves of the fabricated composites (S_3).

elongation is increased up to 47.48% for S_2 indicating that the films become more ductile in comparison with pure PCF (S_1). The increase in elongation is accompanied by an increase in tensile strength (103.45 MPa). For further addition of GO nanomaterials (10%) within the PCF, a remarkable increase in elongation (40%) and tensile strength (44%) is clearly visible. This could happen due to the formation of more compact network that generated from the addition of GO nanomaterials within the PCF. This trend has been also reported in the literature for GO filled bionanocomposite films [47, 48] Such improvements confirm that GO has significant impacts on PCF. However, further addition of GO (higher than 10%) results in the decrease of tensile strength and elongation at break. At 15% GO addition, S_4 has 113.49 MPa tensile strength and percentage of elongation as 58.75% which are less than the tensile and elongation properties of S_3 (10% GO). In addition, low tensile strength as well as elongation percentage are noticed for S_5 (20% GO). So, the gradual decrease of tensile strength and elongation percentage after 10% GO addition in PCF is happened due to the agglomeration of the materials rather than eventual distributed in the composite matrix, and the same phenomena was also observed in earlier studies [49–51] After all, the percentage of elongation and tensile strength of the PCF with the optimum dose of 10% GO (S_3) is about 66.69% and 149 MPa, which is an increase of 164.64% and 216%, respectively, in compared to control. These phenomenons were also demonstrated in the stress–strain curve of the composites which was presented in Figure 8. The stress–strain curves stated a remarkable improvement in strength and stability for S_3 compared to other composites. The curve for S_3 exhibited a steady rise in stress until reaching the ultimate tensile strength 149 MPa with a strain of 0.67, showcasing the enhanced load-bearing capacity of the composite. Furthermore, the S_3 composite material displayed exceptional resilience, with minimal deformation even under prolonged stress, highlighting its durability and suitability for demanding applications [47, 48]. In apparently, the large aspect ratio of GO is responsible for the significant reinforcement impact on the mechanical properties of the PCF. However, it was observed that incorporation of GO nanomaterials into PCF increased not only the tensile strength but also the percentage of elongation, which makes the fabricated films strong and flexible and make it preferable for the packaging industries.

3.9. Mechanical Properties of Various Composite Materials. The comparison of mechanical properties of fabricated composite along with other previous studies is shown in Table 3. The data obtained from this research represented better results in comparison with other studies. Almost similar type of tensile strength (148.70 MPa) and elongation (62.90%) were found for polyacrylonitrile with rGO [29]. Besides, the mechanical properties of fabricated composite film were found better than the previous studies with industrial flax linens incorporated graphene [56]. Incorporation of graphene in composite fabrication creates strong interfacial interaction with the collagen matrix of leather fiber. Better mechanical properties of the fabricated composite were found because of the large surface area as well as high interfacial contact area of graphene nanosized particles [14]. In respect of fiber, the strength of the prepared composite depends on the difference of fiber, length of the fiber, and the ratio of fiber used. The elongation percentage of the composite also depends on the matrix and compatibilizer/binder used for the preparation of the composite. The elongation percentage of the composite prepared from rice straw with GO confirmed better elongation percentage than this study. There were differences in matrix and fiber–matrix ratio between this investigation and the study with rice straw-GO composite [52]. Variation of mechanical properties depends on different types of reinforcement and matrix, composition ratio, and the method of fabrication [48]. According to the discussion, incorporation of graphene with leather fiber in fabricating composites confirmed better mechanical properties to utilize in future applications.

4. Conclusions

High-performance biocomposite films were prepared by blending PCF incorporated with GO by simple solution mixing method. The PCF and GO were effortlessly mixed in water solution with the assistance of PVP compatibilizer. Tensile strength and elongation of composite films with 10% GO were increased by 216% and 164.64%, respectively. In addition, surface morphology and bonding of PCF/GO composite films were ensured through SEM and FTIR. Consequently, the thermal stability of PCF/GO composite films was improved, which was confirmed by TGA. Subsequently, 64% of gas barrier properties and 60% of biodegradable properties were improved for PCF/GO biocomposite films compared to PCF alone. Therefore, the as-prepared biocomposite films with features of high strength and good flexibility will have potential applications as a promising packaging material. This study advocates a unique application of post-consumption waste leather fiber in producing cost-effective, biodegradable, and environmental friendly packaging materials

Table 3: Comparison of mechanical properties of composites with other relevant studies.

Sample name	Tensile strength (MPa)	Elongation (%)	Reference
Postconsumed leather fiber with GO (90 : 10)	149.00	69.66	This study
Rice straw with GO (90 : 10)	50.00	100.00	[52]
Latex with buffing dust and jeans cotton (80 : 20)	6.56	29.98	[53]
Buffing dust with natural rubber with (40 : 60)	13.80	5.80	[54]
Dyed trimmings with jute fiber (50 : 50)	52.67	13.89	[47]
Finished leather fiber with coconut fiber (55 : 45)	5.88	5.62	[55]
Hibiscus cannabinus with GNP (85 : 15)	20.00	4.75	[56]
Finished leather fiber with sisal fiber (60 : 40)	9.08	7.73	[57]
Finished leather scraps with palm fiber (70 : 30)	8.30	3.66	[58]
Polyacrylonitrile with rGO (95 : 5)	148.70	62.90	[29]
Finished waste leather with enset fiber (90 : 10)	2.91	27.84	[7]
Industrial flax linens with graphene (75 : 25)	129.50	1.00	[59]

exemplifying a waste-to-products approach. As well as this research will be a future motivation for investigating the impact of various compatibilizers and additives on improvements of film properties such as flexibility, strength, and biodegradability.

Data Availability

The data are not publicly available due to privacy or ethnic restrictions. The datasets used and/or analyzed during this study are available from the corresponding author on reasonable request.

Additional Points

Highlights. (i) Recycling of postconsumed footwear leather waste to diminish pollution load. (ii) Uniform distribution and the interfacial bonding between GO layers and the host matrix increase physicochemical properties. (iii) GO blocks the gas molecules diffusion, which results in improved gas barrier properties. (iv) The use of fossil materials can be reduced by utilizing PCF/GO-based biocomposites as packaging material.

Conflicts of Interest

The authors declare that they have no conflicts of interest.

Authors' Contributions

Rashedul Islam conducted experimentation in the laboratory. Md Ashikur Rahaman Noyon and Thuhin Kumar Dey analyzed and interpreted the experimental data. Rajasekar Rathanasamy and Moganapriya Chinnasamy characterized the sample. Mamun Jamal reviewed the manuscript. Md. Elias Uddin performed the idea generation, evaluation, and interpreted of overall experimentation. All authors participated in writing the manuscript; read and approved the final manuscript.

Acknowledgments

This study was supported by Research and Extension (R&E), Khulna University of Engineering & Technology, Khulna, Bangladesh (2021–2022).

References

[1] T. Staikos and S. Rahimifard, "Post-consumer waste management issues in the footwear industry," *Proceedings of the Institution of Mechanical Engineers, Part B: Journal of Engineering Manufacture*, vol. 221, no. 2, pp. 363–368, 2007.

[2] V. John Sundar, J. Raghavarao, C. Muralidharan, and A. B. Mandal, "Recovery and utilization of chromium-tanned proteinous wastes of leather making: a review," *Critical Reviews in Environmental Science and Technology*, vol. 41, no. 22, pp. 2048–2075, 2011.

[3] T. Staikos and S. Rahimifard, "An end-of-life decision support tool for product recovery considerations in the footwear industry," *International Journal of Computer Integrated Manufacturing*, vol. 20, no. 6, pp. 602–615, 2007.

[4] R. Temsch and M. Marchich, "Unido programs funded by Austria to strengthen the leather sector in Uganda," p. 68, US/UGA/92/200, US/UGA/96/300, 2002.

[5] V. Mittal, "Functional polymer nanocomposites with graphene: a review," *Macromolecular Materials and Engineering*, vol. 299, no. 8, pp. 906–931, 2014.

[6] M. A. R. Noyon, T. K. Dey, M. Jamal, R. Rathanasamy, M. Chinnasamy, and M. E. Uddin, "Fabrication of LLDPE based biodegradable composite incorporated with leather shavings and buffing dust: an approach for waste management," *Journal of Applied Polymer Science*, vol. 139, no. 47, Article ID e53184, 2022.

[7] A. Teklay, G. Gebeyehu, T. Getachew, T. Yaynshet, and T. P. Sastry, "Preparation of value added composite boards using finished leather waste and plant fibers—a waste utilization effort in Ethiopia," *Clean Technologies and Environmental Policy*, vol. 19, pp. 1285–1296, 2017.

[8] D. Masilamani, V. Srinivasan, R. K. Ramachandran, A. Gopinath, B. Madhan, and P. Saravanan, "Sustainable packaging materials from tannery trimming solid waste: a new paradigm in wealth from waste approaches," *Journal of Cleaner Production*, vol. 164, pp. 885–891, 2017.

[9] Y. Du, S. Z. Shen, K. Cai, and P. S. Casey, "Research progress on polymer–inorganic thermoelectric nanocomposite materials," *Progress in Polymer Science*, vol. 37, no. 6, pp. 820–841, 2012.

[10] T. Premkumar and K. E. Geckeler, "Graphene–DNA hybrid materials: assembly, applications, and prospects," *Progress in Polymer Science*, vol. 37, no. 4, pp. 515–529, 2012.

[11] K. V. Maheshkumar, K. Krishnamurthy, P. Sathishkumar et al., "Research updates on graphene oxide-based polymeric nanocomposites," *Polymer Composites*, vol. 35, no. 12, pp. 2297–2310, 2014.

[12] S. Zhang, H. Wang, J. Liu, and C. Bao, "Measuring the specific surface area of monolayer graphene oxide in water," *Materials Letters*, vol. 261, Article ID 127098, 2020.

[13] P. K. Panda, P. Dash, J.-M. Yang, and Y.-H. Chang, "Development of chitosan, graphene oxide, and cerium oxide composite blended films: structural, physical, and functional properties," *Cellulose*, vol. 29, pp. 2399–2411, 2022.

[14] H. Kim, A. A. Abdala, and C. W. Macosko, "Graphene/polymer nanocomposites," *Macromolecules*, vol. 43, no. 16, pp. 6515–6530, 2010.

[15] J. S. Jayan, K. Pal, A. Saritha, B. D. S. Deeraj, and K. Joseph, "Graphene oxide as multi-functional initiator and effective molecular reinforcement in PVP/epoxy composites," *Journal of Molecular Structure*, vol. 1230, Article ID 129873, 2021.

[16] S. Natarajan, R. Rathanasamy, S. K. Palaniappan, S. Velayudham, H. B. Subburamamurthy, and K. Pal, "Comparison of MA-g-PP effectiveness through mechanical performance of functionalised graphene reinforced polypropylene," *Polímeros*, vol. 30, no. 3, Article ID e2020035, 2020.

[17] S. Stankovich, D. A. Dikin, R. D. Piner et al., "Synthesis of graphene-based nanosheets via chemical reduction of exfoliated graphite oxide," *Carbon*, vol. 45, no. 7, pp. 1558–1565, 2007.

[18] M. El Achaby, F. Z. Arrakhiz, S. Vaudreuil, E. M. Essassi, and A. Qaiss, "Piezoelectric β-polymorph formation and properties enhancement in graphene oxidePVDF nanocomposite films," *Applied Surface Science*, vol. 258, no. 19, pp. 7668–7677, 2012.

[19] M. Aqlil, A. Moussemba Nzenguet, Y. Essamlali, A. Snik, M. Larzek, and M. Zahouily, "Graphene oxide filled lignin/starch polymer bionanocomposite: structural, physical, and mechanical studies," *Journal of Agricultural and Food Chemistry*, vol. 65, no. 48, pp. 10571–10581, 2017.

[20] N. Mahmoudi, F. Ostadhossein, and A. Simchi, "Physicochemical and antibacterial properties of chitosan-polyvinylpyrrolidone films containing self-organized graphene oxide nanolayers," *Journal of Applied Polymer Science*, vol. 133, no. 11, Article ID 43194, 2016.

[21] M. Voronova, N. Rubleva, N. Kochkina, A. Afineevskii, A. Zakharov, and O. Surov, "Preparation and characterization of polyvinylpyrrolidone/cellulose nanocrystals composites," *Nanomaterials*, vol. 8, no. 12, Article ID 1011, 2018.

[22] A. M. Pandele, M. Ionita, L. Crica, S. Dinescu, M. Costache, and H. Iovu, "Synthesis, characterization, and in vitro studies of graphene oxide/chitosan–polyvinyl alcohol films," *Carbohydrate Polymers*, vol. 102, pp. 813–820, 2014.

[23] P. K. Panda, K. Sadeghi, and J. Seo, "Recent advances in poly (vinyl alcohol)/natural polymer based films for food packaging applications: a review," *Food Packaging and Shelf Life*, vol. 33, Article ID 100904, 2022.

[24] C. Rodríguez-González, A. L. Martínez-Hernández, V. M. Castaño, O. V. Kharissova, R. S. Ruoff, and C. Velasco-Santos, "Polysaccharide nanocomposites reinforced with graphene oxide and keratin-grafted graphene oxide," *Industrial & Engineering Chemistry Research*, vol. 51, no. 9, pp. 3619–3629, 2012.

[25] M. E. Uddin, T. Kuila, G. C. Nayak, N. H. Kim, B.-C. Ku, and J. H. Lee, "Effects of various surfactants on the dispersion stability and electrical conductivity of surface modified graphene," *Journal of Alloys and Compounds*, vol. 562, pp. 134–142, 2013.

[26] M. J. Ferreira and M. F. Almeida, "Recycling of leather waste containing chromium—a review," *Materials Science Research Journal*, vol. 5, no. 4, pp. 327–381, 2011.

[27] T. Kuila, S. Bose, C. E. Hong et al., "Preparation of functionalized graphene/linear low density polyethylene composites by a solution mixing method," *Carbon*, vol. 49, no. 3, pp. 1033–1037, 2011.

[28] L. R. Chiappero, S. S. Bartolomei, D. A. Estenoz, E. A. B. Moura, and V. V. Nicolau, "Lignin-based polyethylene films with enhanced thermal, opacity and biodegradability properties for agricultural mulch applications," *Journal of Polymers and the Environment*, vol. 29, pp. 450–459, 2021.

[29] M. E. Uddin, R. K. Layek, N. H. Kim, D. Hui, and J. H. Lee, "Preparation and properties of reduced graphene oxide/polyacrylonitrile nanocomposites using polyvinyl phenol," *Composites Part B: Engineering*, vol. 80, pp. 238–245, 2015.

[30] K. Nakagawa and M. Sugita, "Spectroscopic characterisation and molecular weight of vegetable tannins," *Journal of the Society of Leather Technologists and Chemists*, vol. 83, no. 5, pp. 261–264, 1999.

[31] P. Macheroux, "UV–visible spectroscopy as a tool to study flavoproteins," in *Flavoprotein Protocols*, S. K. Chapman and G. A. Reid, Eds., vol. 131 of *Methods in Molecular Biology*, Humana Press, 1999.

[32] J. S. Jayan, A. Saritha, B. D. S. Deeraj, and K. Joseph, "Triblock copolymer grafted graphene oxide as nanofiller for toughening of epoxy resin," *Materials Chemistry and Physics*, vol. 248, Article ID 122930, 2020.

[33] M. E. S. Mirghani, Y. B. Che Man, H. M. Salleh, and I. Jaswir, "Rapid authentication of leather and leather products," *Advances in Natural and Applied Sciences*, vol. 6, no. 5, pp. 651–660, 2012.

[34] F. Woldesenbet, A. P. Virk, N. Gupta, and P. Sharma, "Biobleaching of mixed wood kraft pulp with alkalophilic bacterial xylanase, mannanase and laccase-mediator system," *Journal of Microbiology and Biotechnology Research*, vol. 3, no. 4, pp. 32–41, 2013.

[35] K. J. Payne and A. Veis, "Fourier transform IR spectroscopy of collagen and gelatin solutions: deconvolution of the amide I band for conformational studies," *Biopolymers*, vol. 27, no. 11, pp. 1749–1760, 1988.

[36] M. H. Alhaji, E. N. Oparah, M. K. Yakubu et al., "Production, properties and applications of cellulose/waste leather buff composite (WLB) for environmental sustainability and recyclability," *Journal of Chemical Society of Nigeria*, vol. 46, no. 3, 2021.

[37] P. Thanikaivelan, T. N. Narayanan, B. K. Gupta, A. L. M. Reddy, and P. M. Ajayan, "Nanobiocomposite from collagen waste using iron oxide nanoparticles and its conversion into magnetic nanocarbon," *Journal of Nanoscience and Nanotechnology*, vol. 15, no. 6, pp. 4504–4509, 2015.

[38] S. S. Banerjee, I. Ramakrishnan, and B. K. Satapathy, "Modification of polydimethylsiloxane with polyvinylpyrrolidone: influence of reinforcing filler on physico-mechanical properties," *Polymer Engineering & Science*, vol. 56, no. 5, pp. 491–499, 2016.

[39] K. V. M. Kumar, K. Krishnamurthy, R. Rajasekar, P. S. Kumar, K. Pal, and G. C. Nayak, "Influence of graphene oxide on the static and dynamic mechanical behavior of compatibilized polypropylene nanocomposites," *Materials Testing*, vol. 61, no. 10, pp. 986–990, 2019.

[40] L. N. Zhou, H. Zhao, Y. Liu et al., "Synthesis of graphene oxide frameworks and their application in electrocatalytic preparation of hydrogen peroxide," *Advanced Materials Research*, vol. 1090, pp. 43–49, 2015.

[41] D. Dutta, R. Hazarika, P. D. Dutta, T. Goswami, P. Sengupta, and D. K. Dutta, "Synthesis of Ag–Ag_2S Janus nanoparticles supported on an environmentally benign cellulose template and their catalytic applications," *RSC Advances*, vol. 6, no. 88, pp. 85173–85181, 2016.

[42] W. H. Ferreira and C. T. Andrade, "Physical and biodegradation properties of graphene derivatives/thermoplastic starch composites," *Polysaccharides*, vol. 2, no. 3, pp. 582–593, 2021.

[43] F.-J. Wang, Y.-Y. Yang, X.-Z. Zhang, X. Zhu, T.-S. Chung, and S. Moochhala, "Cellulose acetate membranes for transdermal delivery of scopolamine base," *Materials Science and Engineering: C*, vol. 20, no. 1-2, pp. 93–100, 2002.

[44] M. E. Uddin, R. K. Layek, H. Y. Kim, N. H. Kim, D. Hui, and J. H. Lee, "Preparation and enhanced mechanical properties of non-covalently-functionalized graphene oxide/cellulose acetate nanocomposites," *Composites Part B: Engineering*, vol. 90, pp. 223–231, 2016.

[45] H. Kim, P. K. Panda, K. Sadeghi, and J. Seo, "Poly(vinyl alcohol)/hydrothermally treated tannic acid composite films as sustainable antioxidant and barrier packaging materials," *Progress in Organic Coatings*, vol. 174, Article ID 107305, 2023.

[46] K. Park, Y. Oh, P. K. Panda, and J. Seo, "Effects of an acidic catalyst on the barrier and water resistance properties of crosslinked poly (vinyl alcohol) and boric acid films," *Progress in Organic Coatings*, vol. 173, Article ID 107186, 2022.

[47] P. Saikia, T. Goswami, D. Dutta, N. K. Dutta, P. Sengupta, and D. Neog, "Development of a flexible composite from leather industry waste and evaluation of their physico-chemical properties," *Clean Technologies and Environmental Policy*, vol. 19, pp. 2171–2178, 2017.

[48] Y.-B. Li, H.-H. Liu, X.-C. Wang, and X.-X. Zhang, "Fabrication and performance of wool keratin–functionalized graphene oxide composite fibers," *Materials Today Sustainability*, vol. 3-4, Article ID 100006, 2019.

[49] H.-H. Liu, W.-W. Peng, L.-C. Hou, X.-C. Wang, and X.-X. Zhang, "The production of a melt-spun functionalized graphene/poly (ε-caprolactam) nanocomposite fiber," *Composites Science and Technology*, vol. 81, pp. 61–68, 2013.

[50] D. Dhamodharan, V. Dhinakaran, P. N. P. Ghoderao, H.-S. Byun, and L. Wu, "Synergistic effect of cellulose nanocrystals-graphene oxide as an effective nanofiller for enhancing properties of solventless polymer nanocomposites," *Composites Part B: Engineering*, vol. 238, Article ID 109918, 2022.

[51] S. Chinnasamy, R. Rathanasamy, H. K. M. Kumar, P. M. Jeganathan, S. K. Palaniappan, and S. K. Pal, "Reactive compatibilization effect of graphene oxide reinforced butyl rubber nanocomposites," *Polímeros*, vol. 30, no. 3, Article ID e2020032, 2020.

[52] A. Allahbakhsh, "PVC/rice straw/SDBS-modified graphene oxide sustainable nanocomposites: melt mixing process and electrical insulation characteristics," *Composites Part A: Applied Science and Manufacturing*, vol. 134, Article ID 105902, 2020.

[53] A. Islam, Y. Molla, T. K. Dey, M. Jamal, R. Rathanasamy, and M. E. Uddin, "Latex reinforced waste buffing dust-jeans cotton composites and its characterization," *Journal of Polymer Research*, vol. 28, Article ID 322, 2021.

[54] M. I. Ugbaja, F. N. Onuoha, U. Ibeneme, M. I. Uzochukwu, H. Opara, and I. N. Mbada, "Swelling and mechanical behaviour of natural rubber vulcanisate filled with leather wastes (buffing dust) and its modeling," *American Journal of Applied Scientific Research*, vol. 2, no. 2, pp. 6–11, 2016.

[55] R. Senthil, T. Hemalatha, B. S. Kumar, T. S. Uma, B. N. Das, and T. P. Sastry, "Recycling of finished leather wastes: a novel approach," *Clean Technologies and Environmental Policy*, vol. 17, pp. 187–197, 2015.

[56] C. I. Idumah and A. Hassan, "Hibiscus cannabinus fiber/PP based nano-biocomposites reinforced with graphene nanoplatelets," *Journal of Natural Fibers*, vol. 14, no. 5, pp. 691–706, 2017.

[57] A. Teklay, G. Gebeyehu, T. Getachew, T. Yaynshet, and T. P. Sastry, "Conversion of finished leather waste incorporated with plant fibers into value added consumer products—an effort to minimize solid waste in Ethiopia," *Waste Management*, vol. 68, pp. 45–55, 2017.

[58] A. Teklay, G. Gebeyehu, T. Getachew, T. Yayneshet, and T. P. Sastry, "Re-utilization of finished leather waste (scraps) blended with different plant fibers using polymer resins: a waste to wealth approach, of the Ethiopian case," *Innovative Energy & Research*, vol. 7, no. 2, Article ID 194, 2018.

[59] D. Liu, Y. Dong, Y. Liu, N. Ma, and G. Sui, "Cellulose nanowhisker (CNW)/graphene nanoplatelet (GN) composite films with simultaneously enhanced thermal, electrical and mechanical properties," *Frontiers in Materials*, vol. 6, Article ID 235, 2019.